Evaluation of a Wafer Transportation Speed for Propulsion Nozzle Array on Air Levitation System

In-Ho Moon

School of Mechanical Engineering, Sungkyunkwan University,
300 Chunchun-dong, Jangan-ku, Suwon 440-746, Korea

Young-Kyu Hwang*

School of Mechanical Engineering, Sungkyunkwan University,
300 Chunchun-dong, Jangan-ku, Suwon 440-746, Korea

A transportation system of single wafer has been developed to be applied to semiconductor manufacturing process of the next generation. In this study, the experimental apparatus consists of two kinds of track, one is for propelling a wafer, so called control track, the other is for generating an air film to transfer a wafer, so called transfer track. The wafer transportation speed has been evaluated by the numerical and the experimental methods for three types of nozzle position array (i.e., the front-, face- and rear-array) in an air levitation system. Test facility for 300 mm wafer has been equipped with two control tracks and one transfer track of 1500 mm length from the starting point to the stopping point. From the present results, it is found that the experimental values of the wafer transportation speed are well in agreement with the computed ones. Namely, the computed values of the maximum wafer transportation speed $V_{\max}$ are slightly higher than the experimental ones by about 15~20%. The disparities in $V_{\max}$ between the numerical and the experimental results become smaller as the air velocity increases. Also, at the same air flow rate, the order of wafer transportation speeds is : $V_{\max}$ for the front-array $>$ $V_{\max}$ for the face-array $> V_{\max}$ for the rear-array. However, the face-array is rather more stable than any other type of nozzle array to ensure safe transportation of a wafer.

Key Words : Wafer Transfer, Air Levitation, Transportation Speed, Propulsion Nozzle, Single Substrate Transfer

Nomenclature

A : Propulsion nozzle area [m²]
C_D : Drag coefficient
C_p : Propulsive force coefficient
d : Propulsion nozzle diameter [m]
h : Floating height [m]
l : Boundary layer [m]
L : Wafer moving distance [m]
L_1 : Distance from starting point to V_1 [m]

L_2 : Distance from starting point to V_2 [m]
$L_{\max}$: Distance from starting point to $V_{\max}$ [m]
q : Air flow rate per one nozzle [m³/s]
R : Radius of wafer [m]
R_v : Gradient of wafer speed
    $[=(V_2-V_1)/(L_2-L_1), 1/s]$
S : Cross-sectional area of wafer [m²]
V : Wafer transportation speed [m/s]
V_1 : Wafer transportation speed at L_1 [m/s]
V_2 : Wafer transportation speed at L_2 [m/s]
V_a : Air velocity of propulsion nozzle [m/s]
$V_{\max}$: Maximum wafer speed at the end of acceleration region [m/s]

Greek Symbols

θ : Angle of inclination of propulsion nozzle

* Corresponding Author,
  E-mail : ykhwang@skku.edu
  TEL : +82-31-290-7437; **FAX** : +82-31-290-5889
  School of Mechanical Engineering, Sungkyunkwan University, 300 Chunchun-dong, Jangan-ku, Suwon 440-746, Korea. (Manuscript **Received** October 10, 2005; **Revised** June 13, 2006)

[degree]
μ : Viscosity of air [Pa·s]
ν : Kinematic viscosity [m²/s]
ρ : Density of air [kg/m³]
τ_0 : Shearing stress of air [N/m²]

1. Introduction

In recent years, a new era of display has brought continuous development of personal computers and information technology industry, and increasing demand on semiconductors and flat panel displays (FPDs). The demand for the importance of cost-effectiveness is increased to ensure competitiveness in the industry, and cost-effective processes are also required of clean room facilities (Oh, 1991). An automated material handling system is being used as a method to reduce manufacturing cost in the semiconductor and FPDs manufacturing processes. We are considering switch-over from the traditional cassette system to single-substrate transfer system to reduce raw materials of stocks in the processing line.

According to the current studies (Cho, 2001 ; Hayashi, 2002), the adoption of single-substrate transfer system can give a opportunity to reduce stocks in the processing line, and significantly shortening the 'Turn Around Time' as much as 80%. The single-substrate transfer systems can be subcategorized in methods of wafer levitation by the compressed clean air, magnetic levitation of vehicles, and wafer transfer by linear motors. Even though none of the three systems are applied currently to commercial operation, several manufacturer in Korea have made efforts to implement a single-substrate transfer system for mother glass in the liquid crystal display (LCD) manufacturing process.

As the first research on the wafer transfer system, Paivanas and Hassan (1979) in IBM proposed the wafer transfer system based on a lubricating film of air as means for levitating and moving wafers. In their study, both wafer transportation and positioning are achieved with the air film, operating in conjunction with special control device techniques. Toda et al.(1992 ; 1993) made a wafer transfer system by air levitation, and they

enhanced transfer characteristics of 6 inch wafer by improving the system of Paivanas and Hassan (1979). In their study, it takes less than 15 sec. from propelling to stopping a 12 inch wafer in the 800 mm long wafer transport track. Moon and Hwang (2004) performed the theoretical study on the transportation of a wafer to a specific position by compressed air, and they suggested that the propulsive force coefficient required for the design of an air levitation system.

It is very important for the process ability in a single-substrate transfer system to control properly the wafer speed. Our study is the first to introduce the transportation speed of a wafer which corresponds to the three types of nozzle position array (i.e., the front-, face- and rear-array) in an air levitation system. We have investigated the characteristics of both behaviors of the propulsion speed and the transportation speed of a 300 mm wafer with respects to the three types of nozzle position array associated with the air velocities of propulsion nozzles.

2. Wafer Propulsion

A wafer transportation system is consisted of two control tracks and one transfer track. The mechanism of a wafer transportation is shown in Fig. 1 and wafer propulsion nozzles are inclined towards the direction of wafer moving at vertical angle θ. The floating wafer is transported by the tangential force component F_x, and exerted by the dynamic pressure as shown in Fig. 1. And this pressure is generated by impinging air jets, with vertical angle θ, of propulsion nozzles. If the wafer mass is m, and wafer speed is V, the tangential force component F_x can be calculated as follows (Toda et al., 1992 ; 1993).

$$m\frac{dV}{dt}=F-D_1-D_2-D_3 \qquad (1)$$

$$F=N\times F_x \qquad (2)$$

$$F_x=\frac{1}{2}C_p\left(\frac{\rho q^2}{A}\right)\sin\theta \qquad (3)$$

where A is the cross sectional area of nozzle, C_p

is the propulsive force coefficient, N is the number of nozzles covered by a wafer, q is the supplied air flow rate per each nozzle, and ρ is the density of air.

The resistance forces of the wafer motion are classified into D_1, D_2 and D_3. The force D_1 is the frictional resistance acting on upper surface, D_2 is the drag force acting on edge, and D_3 is frictional resistance acting on underside of a wafer. To calculate the linear speed of wafer from the equation of motion, D_1, D_2 and D_3 can be calculated by the following equations.

$$D_1 = 2 \int_0^R \left[\int_0^{2\sqrt{r(2R-r)}} \right] dr \qquad (4)$$

$$D_2 = C_D \frac{\rho V^2}{2} S \qquad (5)$$

$$D_3 = \frac{D^2}{4} \mu \frac{V}{h} \qquad (6)$$

where C_D is the drag coefficient, D is the diameter of wafer, h is the floating height of a wafer, l is the boundary layer, R is the radius of wafer, S is the cross-sectional area of wafer, μ is the viscosity of air, and the shearing stress of air is $\tau_0 = 0.332 \, \mu V \sqrt{V/\nu l}$.

In this study, under the condition of the wafer speed is less than 1 m/s, the value of drag coefficient $C_D = 2.05$ is chosen for the numerical calculation of Eq. (5) (Son et al., 1992).

3. Wafer Transportation Speed

3.1 Numerical analysis model

An analysis model for wafer speed is equipped with two control tracks of 500 mm length and one transfer track of 1000 mm length as illustrated in Fig. 2. The three types of nozzle position array of propulsion nozzles are illustrated in Fig. 3, which are classified into the front-array (a), rear-array (b) and face-array (c) in Fig. 3. The propulsion nozzles corresponding to the front-array are positioned at front side toward the direction of wafer
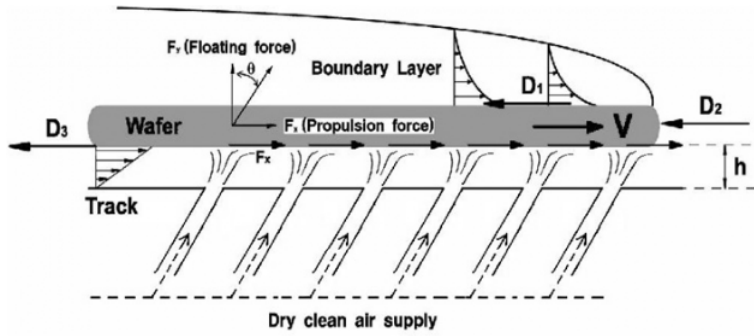

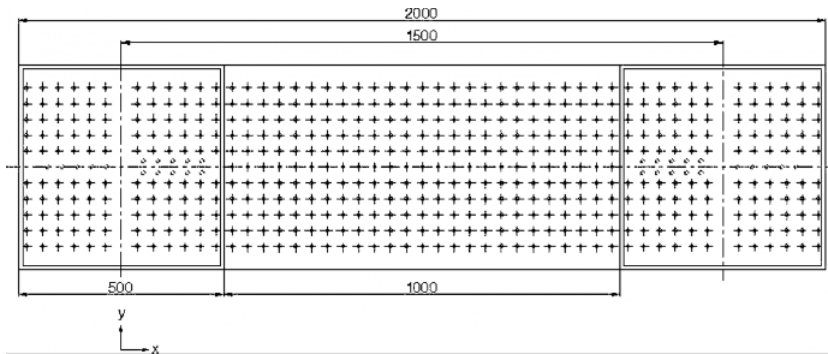**Fig. 1** Mechanism of wafer transportation

Fig. 2 Arrangement of tracks and nozzles for Analysis model

transfer from the center of control track (see Fig. 3(a)). The propulsion nozzles corresponding to the rear-array are positioned at rear side of the
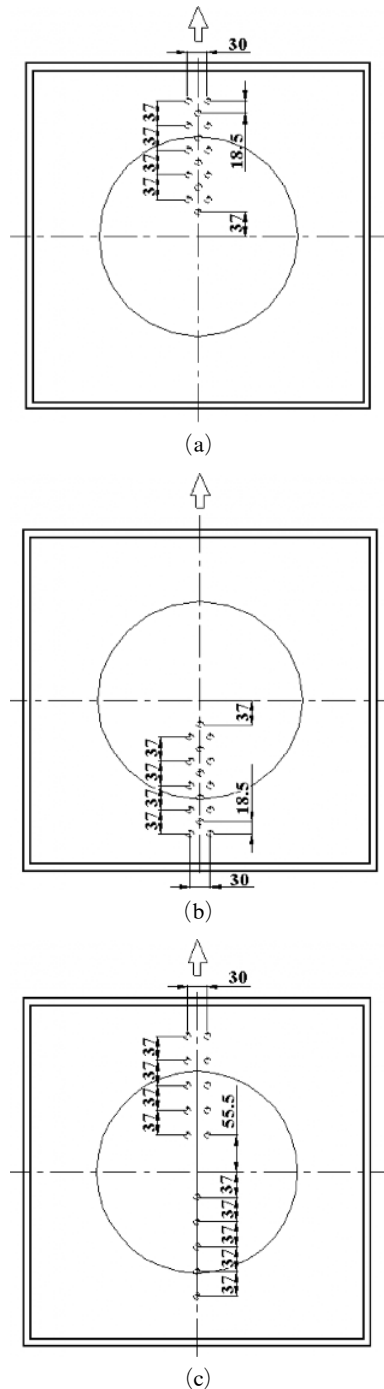

(a)

(b)

(c)

Fig. 3 Control track of position array for (a) front-array, (b) rear-array and (c) face-array

control track center (see Fig. 3(b)). And the propulsion nozzles corresponding to the face-array are distributed at front and rear side of the control track (see Fig. 3(c)). The inclined angle of propulsion nozzle is 45° and nozzle pitch is 37 mm. Total number of propulsion nozzles are 15. But, when the wafer starts, a number of nozzles by which the propulsive forces are acting on the wafer become only 10. In the calculation of wafer transportation speed, the parameters are given as follows : diameter of wafer $D=300$ mm, weight of wafer $W=127$ g, floating height of wafer $h=0.4$ mm, propulsion nozzle diameter $d=0.8$ mm, propulsion nozzle angle $\theta=45°$ and air velocity of propulsion nozzle $V_a=50\sim150$ m/s, respectively. The propulsive force coefficient C_p obtained by the experimental and numerical study of Moon and Hwang (2004), is given in Table 1 for wafer speed calculation.

3.2 Numerical method

The governing equation for a wafer speed is obtained by Eq. (1). This partial differential equation can be discretized in time as follows (Ferziger and Peric, 1996).

$$m\frac{dV}{dt}=F_x-D_1-D_2-D_3=RES \qquad (7)$$

This leads to the following second order discretization by Adams-Bashforth method.

$$m\frac{V^{n+1}-V^n}{\Delta t}=\frac{3}{2}(RES)^n-\frac{1}{2}(RES)^{n-1} \quad (8)$$

or, rearranged by new time step (n+1)st value :

$$V^{n+1}=V^n+\frac{\Delta t}{m}\left[\frac{3}{2}(RES)^n-\frac{1}{2}(RES)^{n-1}\right] (9)$$

In this method, if the time step (n)th value of right side is known, new time step (n+1)st value can be calculated. The number of propulsion

Table 1 Propulsive force coefficient C_p at various V_a

d (mm)	V_a (m/s)	C_p
	50	1.4473
0.8	100	1.2405
	150	1.1848

nozzles is changed in accordance with the wafer movement. If the wafer speed is less then 10^{-7} m/s, the calculation of wafer speed is terminated.

3.3 Numerical results

The computed values of the wafer speed corresponding to the three types of position array of propulsion nozzles are shown in Figs. 4~6 at the propulsion air velocity 50, 100, and 150 m/s, respectively. The maximum wafer speed V_{max} is defined as the highest speed at the end of acceleration region. Also, the distance corresponding to the highest speed L_{max} is defined as the length from the starting point to the point at which the highest wafer speed rises. The values of V_{max} and L_{max} which correspond to the front-, face-, and rear-array are summarized in Table 2. In both cases of the front- and the face-array, the respec-

tive values of L_{max} are about 350 mm. In case of the rear-array, $L_{max} \cong 110$ mm is relatively very short. When the values of V_{max} corresponding to the face- and the rear-array are compared to the reference speed corresponding to the front-array, those are about 85% for the face-array and 40% for the rear-array, respectively. However, each curve of wafer speeds has the similar pattern of three typical parts. Namely, those are the nonlinear acceleration part near the starting point, the linear deceleration part for most of moving distance, and the nonlinear deceleration part near the stopping point, regardless the magnitude of the air velocity and the types of nozzle position array (see Figs. 4~6). Finally, at the same air velocity of propulsion nozzle, the value of V_{max} corresponding to the front-array is predicted to be the highest one.

Table 2 Comparison of the numerical and the experimental values of V_{max} and L_{max} at varies V_a for the three types of position array

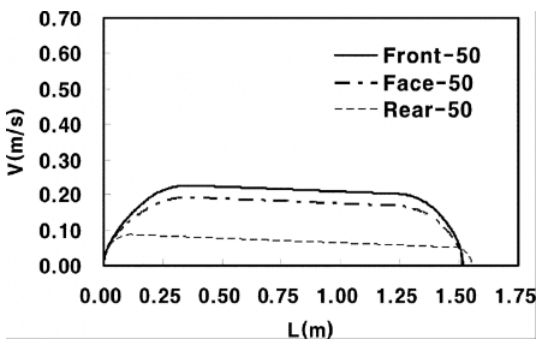| Method \ Scope	V_a (m/s)	V_{max} (m/s)		L_{max} (mm)	
		Cal.	Exp.	Cal.	Exp.
Front-array	50	0.23	0.18	351.5	278.0
	100	0.42	0.35	355.8	302.6
	150	0.62	0.56	362.5	300.6
Face-array	50	0.19	0.16	352.9	319.6
	100	0.36	0.30	356.9	316.0
	150	0.53	0.45	358.1	311.9
Rear-array	50	0.09	0.07	111.6	59.7
	100	0.16	0.14	112.1	85.4
	150	0.24	0.20	114.7	91.6

Fig. 4 Wafer speed V for the three types of position array at V_a=50 m/s
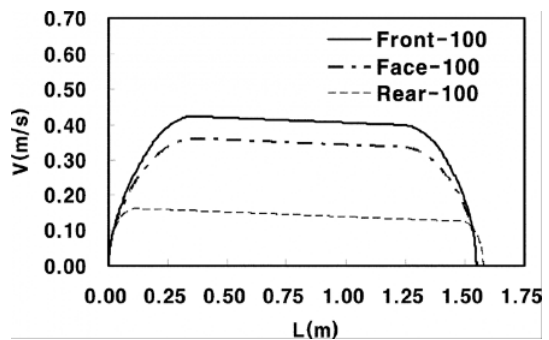

Fig. 5 Wafer speed V for the three types of position array at V_a=100 m/s

Concerning the linear deceleration part in the profile of the wafer speed, an appropriate gradient of wafer speed can be calculated to evaluate the total resistances of D_1, D_2 and D_3 in Eqs. (4) ~ (6). The gradient of wafer speed R_v is defined as follow,

$$R_v = \frac{V_2 - V_1}{L_2 - L_1} \qquad (10)$$

where V_1 and V_2 are the wafer speeds at L_1 and L_2, and the value of L_1 is 550 mm, and L_2 is 850 mm from the wafer starting point, respectively.

The gradients of wafer speed $|R_v|$ are summarized in Table 3. From the present results, it is known that the range of $|R_v|$ is 2.607×10^{-2} ~ 2.814×10^{-2} in proportion to the air velocity. The respective values of $|R_v|$ are 2.681×10^{-2} ~ 2.814×10^{-2} for the front-array, $|R_v| = 2.660 \times 10^{-2}$ ~ 2.795×10^{-2} for the face-array, and $|R_v| = 2.607 \times 10^{-2}$ ~ 2.681×10^{-2} for the rear-array. Both values of $|R_v|$ corresponding to the front- and the face-array are almost same since their difference is less than 2.2×10^{-4}. But, in case of the rear-array, the difference in $|R_v|$ with the front-array is relatively larger by about 7.4×10^{-4} ~
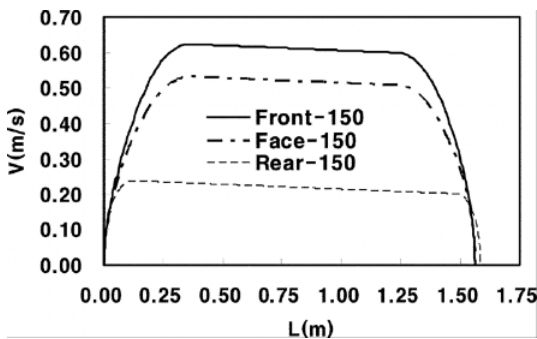

Fig. 6 Wafer speed V for the three types of position array at $V_a = 150$ m/s

Table 3 Values of the gradient $|R_v|$ for the three types of position array

Type V_a (m/s)	Front-array ($\times 10^{-2}$)	Face-array ($\times 10^{-2}$)	Rear-array ($\times 10^{-2}$)
50	2.681	2.660	2.607
100	2.752	2.730	2.643
150	2.814	2.795	2.681

1.3×10^{-3}. These values of $|R_v|$ are necessary to control the wafer motion properly in the air levitation system. It is clear that the value of $|R_v|$ is determined by the linear relation of the wafer speed with the position from the point of maximum wafer speed V_{max}.

4. Experimental Apparatus and Procedure

4.1 Experimental apparatus

The experimental apparatus is consisted of two kinds of track illustrated in Fig. 7. The control tracks installed both side are for propelling a wafer, and the transfer track installed between control tracks is generating an air film for a wafer transfer. The mass flow meter is installed between the control track and valve to measure total mass flow rate of the propulsion nozzles. Before propelling wafer, the floating height of wafer is set up for 0.4 mm. The array types and specifications of propulsion nozzles are all the same as the numerical analysis model. A mean transportation speed of a wafer is measured using a stop watch at the point of 1250 mm from the starting point. An acceleration speed of a wafer is measured using high speed digital camera connected to data acquisition system. The mass flow rate of supply air is controlled by a pressure regulator and mass flow meter. For the purpose of accurate air velocity control, the mass flow rate of compressed air is controlled by a pressure regulator each step, before the experiment starts. When the valve is switched on, compressed air is supplied to the propulsion nozzles and the high speed digital camera is
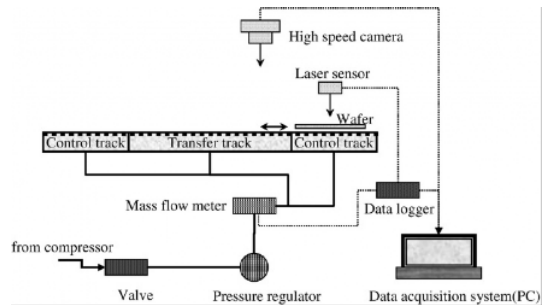

Fig. 7 Schematic diagram of the experimental apparatus

operated to take pictures concurrently.

4.2 Experimental procedure

Experimental procedure to measure the wafer transportation speed is as followed.

(1) Set up the track for measuring nozzle array.
(2) Centering the wafer after the track leveling.
(3) Check the compressed air pressure and mass flow rate.
(4) Switch the main valve on for supply air.
(5) Switch the air supply valve on and digital high speed camera, simultaneously.
(6) Take a sequence of motion pictures to measure the speed of wafer transportation with variable mass flow rate of supply air.
(7) After track shift, change the frame number of camera in accordance with wafer transportation speed, and then, take a sequence of motion pictures.

5. Results and Discussions

5.1 Wafer speed in an acceleration region

A wafer speed in an acceleration region is measured by taking a sequence of motion pictures with a high speed digital camera. Motion pictures of a wafer corresponding to the three types of position array of propulsion nozzles are taken at three given values of air velocity V_a=50, 100, and 150 m/s, respectively, so as to determine the effect of the position array on the wafer speed. At first, the pictures are converted to the wafer speed, and then the respective values for the three types of position array are given in Figs. 8~10.

From the experimental data of wafer speed as shown in Fig. 8, at fixed V_a=50 m/s, the values of the maximum wafer speed are V_{max}=0.18 m/s for the front-array and V_{max}=0.16 m/s for the face-array, respectively. But, V_{max}=0.07 m/s for the rear-array is the lowest speed. Similarly, Fig. 9 designates that at fixed V_a=100 m/s, those are the highest speed of V_{max}=0.35 m/s for the front-array, the next one of V_{max}=0.30 m/s for the face-array, and the lowest one of V_{max}=0.14 m/s for the rear-array, respectively. Also, Fig. 10 shows that at fixed V_a=150 m/s, those are the highest

one of V_{max}=0.56 m/s for the front-array, the next one of V_{max}=0.45 m/s for the face-array, and the lowest one of V_{max}=0.2 m/s for the rear-array, respectively. Consequently, it is clear that the wafer speed strongly depends on the nozzle position array as well as the air velocity of the propulsion nozzles.
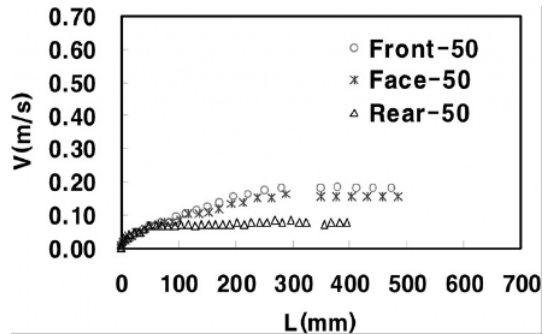

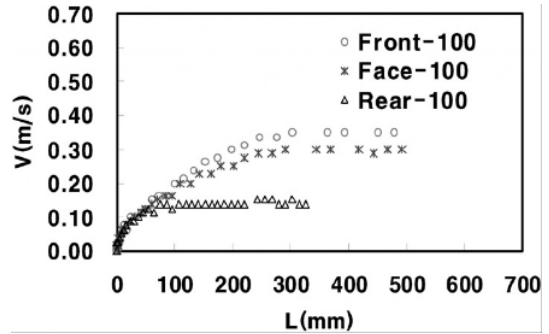Fig. 8   Wafer speed V for the three types of position array at V_a=50 m/s

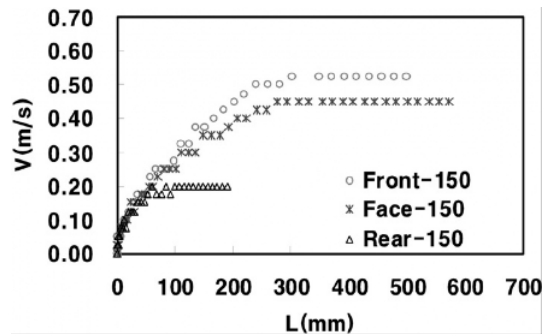Fig. 9   Wafer speed V for the three types of position array at V_a=100 m/s

Fig. 10   Wafer speed V for the three types of position array at V_a=150 m/s

Both the experimental and the computed values of the wafer speed are compared for the three types of position array as shown in Figs. 11~13. The detail values of V_{max} and L_{max} in comparison
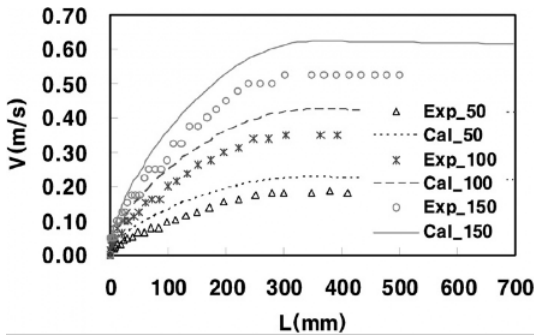

Fig. 11 Comparison of the numerical and the experimental values of wafer speed V for the front-array at various V_a
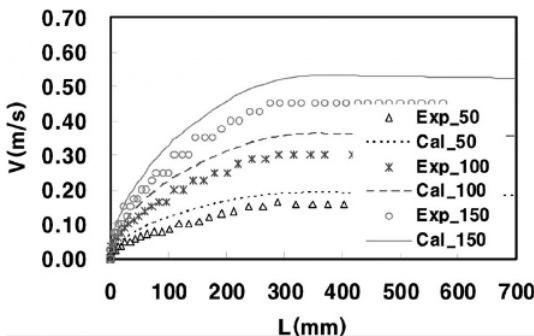

Fig. 12 Comparison of the numerical and the experimental values of wafer speed V for the face-array at various V_a
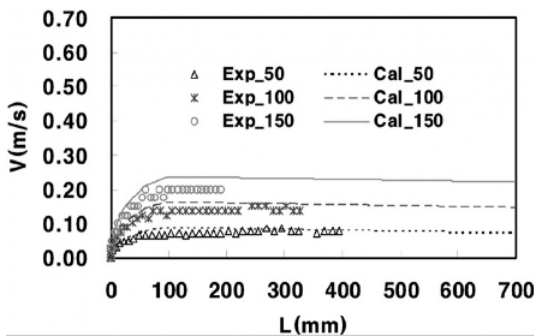

Fig. 13 Comparison of the numerical and the experimental values of wafer speed V for the rear-array at various V_a

of the computed values with the experimental ones are listed in Table 3.

In both cases of the front- and face-array, the computed values of V_{max} and L_{max} are larger than the experimental ones by about 10~20%, as shown in Figs. 11 and 12. However, in case of the rear-array in Fig. 13, the computed values of V_{max} are larger than the experimental ones by about 14~23%, and their values of L_{max} are larger than the experimental ones by about 20~47%, respectively. These disparities between the computed and the experimental values are more significant than those in both cases of the front- and face-array, because the wafer speed is relatively slow. From both the theoretical and the experimental results, the disparities between them in V_{max} and L_{max} become smaller as the air velocity increases. Moreover, the computed curves of wafer speed predict the patterns of the experimental ones with reasonable accuracy regardless of the types of position array. At the same air flow rate, the order of wafer speeds is : V_{max} for the front-array > V_{max} for the face-array > V_{max} for the rear-array. However, the face-array is rather more stable than any other types of nozzle array to ensure safe transportation of a wafer. It is because the face-array produces relatively uniform injection flows around the whole wafer to avoid the unstable movement.

5.2 Mean transportation speed of wafer

The experimental and the theoretical mean transportation speeds of a wafer according to the three types of propulsion nozzle array are illustrated in Fig. 14. In case of the front-array, the corresponding theoretical speed is greater than the experimental one by about 20~23%. In case of the face-array, the theoretical speed is greater than the experimental one by about 15~18%, respectively. But in case of the rear-array, the disparity between the experimental and the theoretical ones is too small to distinguish.

In this result, the mean transportation speeds of wafer are increased linearly in proportion to the air velocities. These disparities between them in the mean transportation speed of a wafer become larger as the air velocity of propulsion nozzle
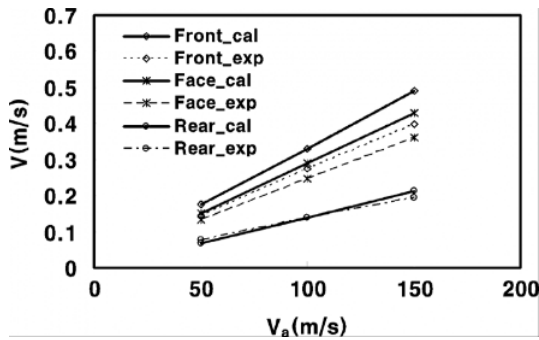
Fig. 14 Comparison of the numerical and the experimental values of mean transportation speed of wafer for the three types of position array at various V_a

increases. First of all, this is mainly because the propelled air gives so significant effect on the floating height of a wafer that its floating height becomes excessively, when the wafer starts. Another reason is that the wafer moving is hindered by strong negative pressure under the wafer caused by induced flow.

6. Conclusions

A single wafer transportation system for handling 300 mm silicon wafers on a lubricating film of air is constructed, and then the wafer speed is not only computed numerically but also measured experimentally with respect to the combination of three types of nozzle position array and various values of the air velocity of propulsion nozzle. The wafer speed is computed by the equation of motion, and it is measured by using a digital high speed camera. It is very important for the process ability in the single-substrate transfer system to control properly wafer transportation speed.

From the present results, at the same air flow rate, the order of wafer speeds is : V_{max} for the front-array $> V_{max}$ for the face-array $> V_{max}$ for the rear-array. The air velocity of propulsion nozzle should be greater than 150 m/s except the rear-array to satisfy the required condition of the wafer speed $V \geq 0.5$ m/s, in actual system. However, the face-array is rather more stable than any other types of nozzle array to ensure safe transportation of a wafer.

The computed values are well in agreement with experimental ones quantitatively. Also, it is found that the computed values of maximum speed of wafer V_{max} are slightly higher than the experimental ones by about 15~20%. In case of the mean transportation speed of wafer, the maximum disparity between the computed and the experimental values is less than 23%.

The disparities in wafer speed between the experimental and the numerical results become larger as the air velocity increases. This is because not only the strong negative pressure caused by induced flow under the wafer but also the floating impact of air are enlarged significantly in accordance with the increase in the air velocity of propulsion nozzles.

Acknowledgements

References

Cho, S. J., 2001, "300 mm Wafer Transportation System for Next Generation," *Air Cleaning Technology* (*in Korean*), Vol. 14, No. 4, pp. 40~59.

Ferziger, J. H. and Peric, M., 1996, *Computational Methods for Fluid Dynamics*, ISBN 3-540-59434-5 Springer-Verlag Berlin Heidelberg New York, pp. 127~143.

Hayashi, T. U. (e-CATS), 2002, "The Revolution of Semiconductor Manufacturer Required Next Eeneration," *Semiconductor Industrial Newspaper Forum*.

Moon, I. H. and Hwang, Y. K., 2004, "Evaluation of a Propulsion Force Coefficients for Transportation of Wafers in an Air Levitation System," *Korean Journal of Air-conditioning and Refrigeration Engineering*, Vol. 16, No. 9, pp. 820~827.

Oh, M. D., 1991, "Ultra-clean Clean Room Technology for GIGA Level Semiconductor," *Transactions of the KSME* (*in Korean*), Vol. 41, No. 6, pp. 32~39.

Paivanas, J. A. and Hassan, J. K., 1979, "Air

Film System for Handling Semiconductor Wafers," *IBM Journal Research and Development*, Vol. 23, pp. 361~375.

Son, B. J., Maeng, J. S. and Lee, S. H., 1992, *Fluid Mechanics, Heejoongdang*, Seoul, Korea, pp. 1108.

Toda, M., Ohmi, M., Nitta, T., Saito, Y., Kanno, Y., Umeda, M., Yagai, M. and Kidokoro, H., 1993, "N$_2$ Tunnel Wafer Transport System," *Proceedings Institute of Environmental Sciences*, pp. 493~499.

Toda, M., Shishido, M., Kanno, Y., Umeda, M., Nitta, T. and Ohmi, T., 1992, "Wafer Transportation Through a Tunnel Filled with Nitrogen Gas," *ICCCS Proceedings*, pp. 173~183.